HHS Public Access

Author manuscript

Hippocampus. Author manuscript; available in PMC 2019 August 01.

Published in final edited form as:

Hippocampus. 2018 August ; 28(8): 568–585. doi:10.1002/hipo.22961.

Hippocampal place cell dysfunction and the effects of muscarinic M_1 receptor agonism in a rat model of Alzheimer's disease

Claire R. Galloway[1], **Kaushik Ravipati**[2], **Suyashi Singh**[2], **Evan P. Lebois**[3], **Robert M. Cohen**[4], **Allan I. Levey**[5], and **Joseph R. Manns**[1]

[1]Department of Psychology, Emory University, Atlanta, GA USA

[2]Neuroscience and Behavioral Biology Program, Emory University, Atlanta, GA USA

[3]Internal Medicine Research Unit, Pfizer Inc. Cambridge, MA, USA

[4]Department of Psychiatry, Emory University, Atlanta, GA USA

[5]Department of Neurology, Emory University, Atlanta, GA USA

Abstract

Alzheimer's disease (AD) is a neurodegenerative disease that disproportionately impacts memory and the hippocampus. However, it is unclear how AD pathology influences the activity of surviving neurons in the hippocampus to contribute to the memory symptoms in AD. One well-understood connection between spatial memory and neuronal activity in healthy brains is the activity of place cells, neurons in the hippocampus that fire preferentially in a specific location of a given environment (the place field of the place cell). In the present study, place cells were recorded from the hippocampus in a recently-developed rat model of AD (Tg-F344 AD) at an age (12–20 months) at which the AD rats showed marked spatial memory deficits. Place cells in the CA2 and CA3 pyramidal regions of the hippocampus in AD rats showed sharply reduced spatial fidelity relative to wild-type (WT) rats. In contrast, spiking activity of place cells recorded in region CA1 in AD rats showed good spatial fidelity that was similar to CA1 place cells in WT rats. Oral administration of the M_1 muscarinic acetylcholine receptor agonist VU0364572 impacted place cell firing rates in CA1 and CA2/3 hippocampal regions but did not improve the spatial fidelity of CA2/3 hippocampal place cells in AD rats. The results indicated that, to the extent the spatial memory impairment in AD rats was attributable to hippocampal dysfunction, the memory impairment was more attributable to dysfunction in hippocampal regions CA2 and CA3 rather than CA1.

Keywords

Acetylcholine; memory; CA1; CA3; dementia

Corresponding author: Joseph Manns, 36 Eagle Row, Atlanta, GA 30332. 404-727-7459. jmanns@emory.edu.

Conflict of Interests: EPL is a named inventor on the following patents and applications relevant to VU0364572: US Pat No 8,697,691; US Pat Appl 20130197027; US Pat Appl 20120088791.

Alzheimer's disease (AD) is a neurodegenerative disease characterized pathologically by accumulation of beta-amyloid (Aβ) plaques and neurofibrillary tangles (NFTs) (Querfurth and LaFerla, 2010). AD is a complex disease that also involves inflammation, oxidative stress, synaptic dysfunction, and cell death (Querfurth and LaFerla, 2010). The pathophysiological basis for the hallmark clinical feature of memory loss remains unclear, but the degree of synaptic dysfunction and cellular loss correlates best with the severity of dementia (Dekosky and Scheff, 1990; Dickson et al., 1995; Terry et al., 1991). The hippocampus is an early target of AD pathology, reflected by Aβ plaques and NFTs, neurodegeneration (i.e., hippocampal atrophy), and functional abnormalities (Braak and Braak, 1995; Chhatwal and Sperling, 2012; Vemuri and Jack, 2010). However, the mechanistic links between AD pathology and hippocampal physiology and function–or dysfunction–are poorly understood.

One well-understood connection between spatial memory and neuronal activity in healthy brains is the activity of place cells, first discovered in the rat hippocampus (O'Keefe and Dostrovsky, 1971). Place cells fire preferentially at a specific location of a given environment (the place field of the place cell) and collectively support cognitive maps (O'Keefe and Nadel, 1978), distinct cell assemblies that can also embed temporal and stimuli-specific information to enable associative and episodic memory in addition to spatial memory (Griffin and Hallock, 2013; Manns et al., 2007; Manns and Eichenbaum, 2009; Moser et al., 2008). Hippocampal place cells also have well-characterized relationships with prominent neuronal oscillations, such as theta rhythms (e.g. Foster and Wilson, 2007; O'Keefe and Recce, 1993), which help coordinate bidirectional interactions with adjacent structures such as the entorhinal cortex (Brun et al., 2008; Jeffery, 2007). Cells with location-specific firing can be found in all the major subregions of the rat hippocampus (dentate gyrus, CA1, CA2, CA3, and subiculum), but most data have come from CA1 and CA3 pyramidal cells (e.g., Knierim et al., 2006; Mizuseki et al., 2012). These data have highlighted anatomical and functional differences between CA1 and CA3, differences that are likely important for understanding memory function and dysfunction. For example, CA3 place cells tend to be more stable (e.g., higher correlation in the location-specific firing between the first and last halves of a given session; Mizuseki et al., 2012), but also more vulnerable to age-related dysfunction (e.g., Wilson et al., 2005). Hippocampal place cell function in healthy rats has also been linked to memory processes that are disproportionately impaired in AD (Gallagher and Koh, 2011; Griffin and Hallock, 2013; Manns and Eichenbaum, 2009; Moser et al., 2008). Thus, the study of CA1 and CA3 place cells in rodent models of AD will likely offer important insights about the memory dysfunction associated with early stages of the disease and help to shed light on how these changes relate to changes reported for age-related memory impairments.

Transgenic mouse models of AD have been invaluable for understanding the disease, and prior studies have reported CA1 place cell dysfunction in several different AD mouse models (e.g. Booth et al., 2016; Cacucci et al., 2008; Cayzac et al., 2015; Cheng and Ji, 2013; Mably et al., 2017; Morrissette et al., 2009; Zhao et al., 2014). However, most studies of place cells in healthy animals have been in rats. Thus, a recently-developed rat model of AD (Tg-F344 AD with human genetic mutations APPSwe and PS1ΔE9; Cohen et al., 2013) has provided a new opportunity to leverage the large rat place cell literature in asking how

the activity of hippocampal neurons relate to spatial memory impairments in AD and how interventions might influence this neuronal activity. As they age, these AD rats gradually develop spatial memory impairments as well as many of the pathological hallmarks of the disease in humans– Aβ plaques, NFTs of hyperphosphorylated tau, neuroinflammation, and eventually cell death (Cohen et al., 2013). Thus, physiological studies of hippocampal neuronal activity in these rats offer an opportunity to connect to the extensive body of work on place cells to understand how AD may influence the activity of surviving cells in a key memory region.

Studying place cells in an AD rat model also permits a direct assessment of new potential drug therapies on memory-related neural activity. AD-related memory loss has been associated with death of cholinergic neurons in the basal forebrain, which is the major supplier of acetylcholine (ACh) to the hippocampus and cortex (Bartus et al., 1982), and many drugs for treating cognitive decline in AD increase ACh levels generally throughout the nervous system (Anand and Singh, 2013). One avenue for pursuing new treatments has been the development of new cholinergic activators that target only a subset of the endogenous ACh receptors (Conn et al., 2009). In particular, the M_1 muscarinic ACh receptor (mAChR) is highly expressed in brain regions important for memory, including the hippocampus, and is less implicated in the dose-limiting peripheral side-effects caused by global ACh activation (Bymaster et al., 2003; Levey et al., 1991). Moreover, a recently-developed M_1 mAChR agonist, VU0364572, improved memory (Digby et al., 2012) and influenced place cells in healthy young rats after acute administration (Lebois et al., 2016), and reduced amyloid pathology and memory deficits in a mouse model of AD after chronic administration (Lebois et al., 2017). Thus, an important question is how acute administration of the M_1 agonist VU0364572 would influence place cell function in a rat model of AD.

The goal of the present study was to characterize the neural correlates of spatial memory dysfunction in a rat model of AD and to ask if oral administration of the M_1 mAChR agonist VU0364572 might ameliorate any such dysfunction. In Experiment 1, we tested memory performance monthly in AD rats and their wild-type (WT) littermates, and found that AD rats developed marked spatial memory impairments by 12 months of age. In Experiment 2, we recorded the activity of hippocampal place cells as 12–20 month-old AD and WT rats completed laps around a circular track after oral administration of either the M_1 agonist VU0364572 or a control vehicle. This age range was selected to occur when the AD rats were known to have a spatial memory impairment (Experiment 1) and amyloid load and tau pathology were present but still increasing (Cohen et al., 2013). Despite showing marked spatial memory impairments, several features of hippocampal place cell activity in AD rats were similar to that of WT rats in the vehicle control condition. Notably, spiking activity of place cells recorded in region CA1 showed good spatial fidelity that was similar to CA1 place cells in WT rats. In contrast, spiking activity of place cells in the CA2 and CA3 pyramidal regions of the hippocampus in AD rats showed sharply reduced spatial fidelity relative to WT rats. Administration of the M_1 agonist VU0364572 impacted place cell firing rates in CA1 and CA2/3 place cells but did not improve the spatial fidelity of CA2/CA3 hippocampal place cells in AD rats.

Experiment 1

Materials and Methods

Subjects—Sixteen female Fisher 344 rats were tested each month from 5–12 months of age. Eight rats expressed the human genetic mutations APP_{Swe} and PS1ΔE9 (Tg-F344 [AD]), and eight rats were WT littermates (F344 [WT]). Female rats were used because, as compared to male rats (and irrespective of whether they were in the AD or WT group), female rats were found in pilot testing to much more readily engage in spontaneous object exploration, a necessary prerequisite for object recognition memory testing (see Procedure). Extensive characterization of AD-related neuropathology for the Tg-F344 (AD) rats is available in Cohen et al. (2013), which reported no sex effects. The rats were kept on a 12-hour light/dark cycle (testing occurred during the light period) and were individually housed with free access to water and food. All experimental procedures were approved by the Institutional Animal Care and Use Committee of Emory University.

Procedure—Memory was tested monthly in each rat from 5–12 months of age using two variants of a widely-used novel object recognition memory task (Clark and Squire, 2010; Ennaceur and Delacour, 1988) that takes advantage of the innate novelty preference of rats (see below for details specific to the object and object-in-location variants). The AD rats were previously found to have impaired spatial memory performance at 16 months of age (Cohen et al., 2013), but time points between 6 and 16 months of age were not previously assessed. Several studies in human AD patients and transgenic rodent models have found that AD may particularly impair spatial associative memory, such as the ability to remember the location of a previously encountered object (Good et al., 2007; Hampstead et al., 2011; Hanaki et al., 2011; Kessels et al., 2010), and thus one variant of that task was an object-in-location spatial recognition memory task.

For both variants of the recognition memory task, all testing was conducted in an open box (91.5 by 91.5 cm wide and 61.0 cm tall) made of wood and painted black. Four Velcro patches (2.5 cm by 2.5 cm) were affixed to the midpoints of the four quadrants of the square floor to secure objects during testing. The objects used in the study ranged in size from approximately 7 by 7 by 7 cm to 17 by 17 by 10 cm and were made from ceramic, wood, plastic, or metal. New objects were used for each test session. One month prior to testing (at 4 months of age) rats were habituated to the testing box by allowing them to spend 10 minutes per day in the box for 3 consecutive days. Approximately one week (4–10 days) prior to testing, rats were habituated again to the box for 10 minutes on a single day. For each subsequent month of testing, rats were re-habituated to the box for 5 minutes 1 day prior to testing. On every testing day, rats were also allowed to spend 5 minutes in the empty box immediately prior to the test session. The floor of the box was cleaned with 100% ethanol after each session. For each month of testing, rats completed two sessions of an object recognition memory task within the same day (elapsed time between sessions ranged from 1 to 3 hours), followed by two sessions of an object-in-location recognition memory task the next day. Every rat was tested by the same experimenter who was blind to the genotype of each rat. Figure 1 shows the testing procedure of example trials for both tasks, and procedures specific to each task are described below.

Object recognition memory task: For the study phase of the object recognition memory task, rats were placed in the testing environment for 3 minutes with two novel objects positioned in two of four possible quadrants of the square floor (different quadrant locations were used across the two trials administered to a rat each month). Rats were then placed back into their home cage for a 2-minute delay between the study and test phase. This delay length was chosen because previous studies have shown that the performance of rats on similar location-based object recognition tasks with comparable delays was sensitive to hippocampal damage (e.g. Save et al., 1992). For the test phase of the task, rats were placed back into the testing environment for 3 minutes with a duplicate of one of the study phase objects (the 'repeated' object) and one novel object. The repeated object occupied the same location as it did in the study phase, and the novel object was positioned in the same location as the object it replaced from the study phase. Assignment of objects and quadrant locations to conditions was counterbalanced across rats.

Object-in-location recognition memory task: For the study phase of the object-in-location recognition memory task, rats were placed into the testing environment for 3 minutes with three novel objects placed in three of four possible quadrants of the square floor (different quadrant locations were used across the two trials administered to a rat each month). Rats were then placed back into their home cage for a 2-minute delay between the study and test phase. For the test phase of the task, rats were placed back into the testing environment with duplicates of each object from the study phase. One of these duplicates was placed in the same location as it had appeared during the study phase (the 'repeated location' object), and two of the duplicates were placed in swapped locations (the 'novel location' objects). Assignment of objects and quadrant locations to conditions was counterbalanced across rats.

Analyses—Each study and test session was digitally recorded (30 frames per second) by a video camera mounted to the ceiling of the testing room. Onset and offset of each bout of object exploration during the test phase were scored separately by an experimenter who was blind to both rat genotype and to which condition an object was assigned (e.g. repeated or novel condition). Object exploration was defined as active exploration (e.g., sniffing and whisking) within 1 cm of the object that excluded chewing or rearing on or nearby the objects. For both tasks, a discrimination index (DI) was calculated from the mean raw exploration times of rats during the test phase as a measure of memory performance (DI = mean novel exploration / ([mean novel exploration + mean repeated exploration]). For each month, the relative memory performance of WT and AD rats was determined by calculating the mean of each rat's DI for both sessions of each task for that month, and then calculating the mean DI across rats of each genotype. For the object-in-location task, the mean exploration of the two objects in novel locations was entered into the DI calculation for that session. Trials in which a rat did not explore the to-be-repeated object (or the to-be-repeated object location for the object-in-location task) during the study phase were excluded from analyses. Trials in which a rat did not explore at least one second across all objects in the test phase were excluded from analyses. Due to the month-to-month variability in mean DI scores for both genotypes (likely attributable to the scores being based on only two trials per month), analyses focused on the 4 month averages to determine age-related differences

between WT and AD rats. Analyses focused on genotype differences between tasks and age groups (5–8 months vs. 9–12 months).

Results

AD rats showed age-dependent spatial memory impairments relative to WT rats—Figure 2 shows memory scores (as DIs; see Materials and Methods) for AD and WT rats on both the object and object-in-location recognition memory tasks. The results are shown for the mean DIs of each genotype across 5–8 months of age and 9–12 months of age. A three-way (2×2×2) mixed-effects ANOVA (age: 5–8 or 9–12 months; task: object or object-in-location; genotype: WT or AD) for DIs revealed that in general all rats performed worse at older relative to younger ages ($F[1,14]=5.78$, $p<0.05$, $\eta_p^2=0.29$). In addition, the effect of genotype on memory performance differed between tasks (genotype x task interaction, $F[1,14]=9.07$, $p<0.01$, $\eta_p^2=0.39$). Accordingly, two additional two-way ANOVAs (age by genotype) were conducted on DIs separately for each task. The results revealed that for object recognition memory, all rats performed worse at older ages relative to younger ages ($F[1,14]=4.7$, $p<0.05$, $\eta_p^2=0.26$), yet AD rats performed similarly to WT rats ($F[1,14]=0.73$, $p=0.41$, $\eta_p^2=0.05$). In contrast, for the object-in-location task, memory performance was worse for AD than WT rats ($F[1,14]=12.32$, $p<0.01$, $\eta_p^2=0.47$), and there was a trend for the effect of genotype to differ across age (age x genotype interaction, $F[1,14]=3.48$, $p=0.08$, $\eta_p^2=0.20$). Moreover, preplanned comparisons revealed that AD rats performed similarly to WT rats at ages 5–8 months ($F[1,14]=0.25$, $p=0.63$, $\eta_p^2=0.02$) but were significantly impaired relative to WT rats at ages 9–12 months ($F[1,14]=8.97$, $p<0.05$, $\eta_p^2=0.39$). Thus, the AD rats showed a memory impairment on the spatial variant of the task by 9–12 months of age.

One potential concern was that AD rats may have spent less time exploring and forming memories of objects relative to WT rats. Although exploration times of objects during the study phase for both tasks declined over the months of testing for both AD and WT rats ($M \pm SEM$: 5–8 months WT=27.2±4.5 s; 9–12 months WT=11.9±2.7 s; 5–8 months AD =28.8±2.0 s; 9–12 months AD=10.7±2.1 s), exploration times during the study phase were similar between AD and WT rats ($F[1,14]=0.54$, $p=0.47$, $\eta_p^2=0.04$). Moreover, the spatial memory impairment of AD rats relative to WT rats at 9–12 months of age remained significant even when study exploration was included as a covariate ($F[1,14]=7.51$, $p<0.05$, $\eta_p^2=0.37$).

One unexplained aspect of the data was the poor performance by the WT rats on the object recognition memory task at 9–12 months of age. These same WT rats performed well at the same age on the object-in-location recognition memory task, which depends in part on having an intact memory of a specific object, and thus the combined data suggest that the WT rats likely were capable of good object recognition memory at this age. In any case, the AD rats showed a clear spatial memory deficit at 9–12 months of age but no evidence that they were impaired relative to WT rats on the non-spatial object task at this age. This finding suggests that brain regions important for spatial memory performance in AD rats are impaired by 9–12 months of age.

Interim Summary—The results of Experiment 1 indicated that AD rats had intact non-spatial and spatial recognition memory at 5–8 months of age but developed a spatial memory impairment relative to WT rats between 9–12 months of age. The goal of Experiment 2 was to record hippocampal place cell activity as a window into the possible neural correlates of the spatial memory deficit observed in relatively early stages of the disease in Experiment 1. Spiking activity of pyramidal neurons from the CA fields of the dorsal hippocampus were recorded as AD and WT rats aged 12–20 months completed laps on a circle track. Spatial correlates of the spiking activity were quantified and compared between AD and WT rats. In addition, an M_1-specific mAChR agonist, VU0364572, was administered to both groups of rats before some recording sessions to assess the potential for M_1 agonism to influence spatial correlates in AD rats.

Experiment 2

Materials and Methods

Subjects—Eighteen female Fisher 344 rats underwent surgery to implant chronic recording tetrodes in the hippocampus (see Surgery and histology below). Nine rats expressed the human genetic mutations APP_{Swe} and PS1ΔE9 (Tg-F344 [AD]), and 9 were wild type (WT) littermates. Eleven rats (7 AD and 4 WT) yielded useable neural data. For these rats, testing occurred when the rats were 12–20 months of age (WT M=15.5, AD M=17.0), an age range at which the AD rats were known to have a spatial memory impairment (Experiment 1) and moderate levels of neuropathology (Cohen et al., 2013). One WT and four AD rats were used in a longitudinal behavioral experiment (Experiment 1) that ended several months prior to Experiment 2. The rats were kept on a 12-hour light/dark cycle (testing occurred during the light period), individually housed with free access to water, and placed on a restricted diet such that they maintained at least 90% of their free-feeding weight. All experimental procedures were approved by the Institutional Animal Care and Use Committee of Emory University.

Drugs—VU0364572 (Lebois et al., 2011), a highly-selective bitopic agonist of the M_1 muscarinic acetylcholine receptor (mAChR), was used to test the effects of M_1 agonism on the spatial fidelity of hippocampal place cells. VU0364572 was chosen for its selectivity for the M_1 mAChR versus other acetylcholine receptors and other off-target proteins (Lebois et al., 2011). In addition, prior studies found that VU0364572 possesed good oral bioavailability and brain penetrance (Lebois et al., 2009; 2011). Further, prior studies established an efficacious range of doses for altering *in vivo* hippocampal function and memory performance in mice and rats (Digby et al., 2012; Galloway et al., 2014; Lebois et al., 2011). Finally, the drug was not found to impact overt behavior (e.g., run or swim speeds) or lead to classic cholinergic side effects in previous studies (Digby et al., 2012; Galloway et al., 2014; Lebois et al., 2011; Lebois et al., 2016). Here, VU0364572 was formulated as an HCl salt in nuclease-free H_2O, and then mixed into strawberry-flavored gelatin for a total volume of 1.2 mL. Thirty minutes prior to each testing session, rats were orally administered either 10 mg/kg M_1 agonist, 30 mg/kg M_1 agonist, or vehicle control. The timing of the drug administration was based upon previously published pharmokinetic data with VU0364572, and selected so that the M_1 allosteric agonist would have a high brain

concentration throughout the testing session (Lebois et al., 2011). The specific 10 mg/kg and 30mg/kg oral doses were selected for their demonstrated efficacy in altering hippocampal function in healthy young rats (Lebois et al., 2016).

Surgery and histology—Each rat underwent surgery using sterile tip technique to affix to the rat's skull a chronic recording assembly with up to 8 tetrodes to record neural activity. A craniotomy was made that centered approximately 3.7 mm posterior and 2.6 mm lateral to the right of bregma. The base of the chronic recording assembly was positioned above this craniotomy so that tetrodes could be independently lowered into the CA1, CA2, and CA3 pyramidal layers of the dorsal hippocampus. Each tetrode consisted of four 12.5 μm nichrome wires. The tips of each tetrode were plated with gold to reduce impedance to 100–200 kΩ at 1 kHz to facilitate the detection of individual units in the hippocampus.

For general analgesia, rats were injected subcutaneously (s.c.) with 2 mg/kg injectable meloxicam before surgery and anesthetized with 1–3% isoflurane in oxygen throughout surgery. Just prior to a midline incision to reveal the skull, up to 0.1 mL of 0.25% bupivacaine with 1:200,000 epinephrine was administered over 2–3 s.c. injections along the scalp as a local anesthetic. Rats were injected s.c. with 2.5 mL of lactated ringers in each the left and right rear haunch for hydration. After the skull was exposed, nine stainless-steel screws were secured along the ridges of the skull to serve as an anchor for the recording assembly. One additional stainless steel screw, soldered to a wire attached to the recording assembly, served as the ground and was secured to the posterior portion of the skull above the cerebellum. The base of the chronic recording assembly was secured to the anchor screws with dental acrylic. During surgery, tetrodes were slowly lowered into the brain until they were roughly 1 mm above the target regions. Topical antibiotics were applied to the incision site, and one to three stiches were used to close the scalp around the base of the implanted device. Before rats were removed from anesthesia, they received a second round of s.c. injections of 5 mL of lactated ringers (2.5 mL in each haunch) to help prevent post-surgery dehydration.

For the first two days after surgery, rats were injected s.c with 1 mg/kg of injectable meloxicam. Rats appearing dehydrated were injected s.c. with 5 mL of lactated ringers (2.5 mL in each haunch). Four rats (all from the AD group), instead of injectable meloxicam and local bupivacaine, received s.c. injections of 0.05 mg/kg buprenorphine prior to surgery followed by an oral dose of 0.75 mL meloxicam (0.5 mg/mL) immediately after the rats began to ambulate after surgery. These same four rats, instead of receiving injectable meloxicam first and second day after surgery, were injected s.c. with 0.05 mg/kg buprenorphine and administered an oral dose of .75 mL meloxicam the first day after surgery, and were administered an oral dose of 0.75 mL meloxicam the second day after surgery. The difference in pre- and post-operative analgesia for these rats was related to changes in recommendations by veterinary staff, and genotype was unknown at the time. All rats were given 1 week to recover, and then tetrodes were slowly lowered 20–80 μm at a time into the target regions of the hippocampus using hallmark electrophysiological cues. In order to minimize movement between sessions, tetrodes were not raised or lowered from 24 hours prior to the first testing session until the rat was euthanized. After testing was completed and just prior to euthanasia, small lesions were made at the tips of recording

electrodes by passing 20–40 μA of direct current for 20 seconds each. After euthanasia, brains were sectioned into 40 μm-thick coronal slices and stained with cresyl violet to confirm tetrode locations based off of marking lesion location.

Procedure—The spatial fidelity of hippocampal place cells was assessed for six consecutive days in each rat. All testing was conducted on a circular track (track outside diameter = 91.5 cm; track width = 7 cm, track height from floor = 81.9 cm) made of wood and painted black. Prior to surgery, rats were trained to complete laps around the circular track for a small food reward (~0.5 g of sprinkles, chocolate flavor) placed at the end of a central stem runway following each lap. After rats reached a pre-surgery criteria of completing 40 laps around the circular track in 40 minutes, rats were implanted with a chronic recording assembly. Rats began testing once they were re-trained to the same lap/minute criteria and as many tetrodes as possible reached their target region in the hippocampus, typically 3–7 weeks after surgery. Only data collected from tetrodes with histologically-confirmed positions in CA1, CA3, or near the CA2/CA3 border during testing sessions were included in the present analysis.

For each day of testing, rats completed one session in which they were administered an oral dose of 10 mg/kg M_1 agonist, 30 mg/kg M_1 agonist, or control vehicle (flavored gelatin) 30 minutes before completing at least 40 laps around the circular track across 35–45 minutes. For each lap, rats exited a central stem runway, completed a clockwise circle, and returned to the center stem for the small food reward. Session 1 and session 6 were always control sessions in which rats were administered only the drug vehicle prior to testing. For sessions 2–5, rats were administered the M_1 agonist VU0364572 in the order of dosages of either 10 mg/kg, 30 mg/kg, 10 mg/kg, 30 mg/kg or 30 mg/kg, 10 mg/kg, 30 mg/kg, 10 mg/kg. The drug sessions were bookended by control sessions to permit the inspection of the data for possible changes across days, such as gradual movements in the positioning of the recording tetrodes.

Data acquisition and analyses—The locomotion of rats during testing was recorded by a digital video camera mounted to the ceiling of the testing environment at a 30 Hz sampling rate (30 frames per second). After testing, the location of a rat's head on each frame was obtained using custom software or manually by a trained experimenter blinded to rat's genotype and drug condition. Light emitting diodes attached to the recording assembly aided the determination of location. Analyses of neural data are described below, and calculations in each case were based on data collected from the two sessions of each drug condition (10 mg/kg VU0364572, 30 mg/kg VU0364572, and control vehicle). In the rare case when only one session was available for a given drug condition (e.g., due to technical computer-related problems), the values represent the calculations for one session rather than the mean of two sessions.

Acquisition of spiking data: Spiking activity of single units was recorded at a sampling rate of 30,000 Hz and filtered at 600–6,000 Hz with the NSpike data acquisition system (nspike.sourceforge.net). After testing, spiking data was manually sorted into putative individual neurons using software that permitted a three-dimensional view of spike waveform characteristics (e.g., spike peak amplitude) across any three wires of a tetrode

(Offline Sorter, Plexon, Dallas, Texas). Putative pyramidal neurons were distinguished from interneurons based on spike waveforms, autocorrelograms, firing rates, and presence of complex spikes, an approach similar to procedures used previously (e.g., Trimper et al., 2017). Too few interneurons were recorded to permit analyses. Timestamps of sorted pyramidal neuron spiking data were then analyzed with custom MATLAB scripts.

Many prior studies have documented differences in patterns of pyramidal neuron spiking activity between hippocampal regions CA1 and CA3 (e.g., Leutgeb and Leutgeb, 2007; Mizuseki et al., 2012; Oliva et al., 2016). The present analyses therefore used data from only tetrodes for which the recording location could be determined by postmortem histology (see Surgery and histology). Specifically, only data from tetrodes that were confirmed to be located in CA1 were used in analyses of CA1 units. Similarly, data from tetrodes confirmed to be located in CA3 were used in analyses of CA3 units. Although the primary goal in distinguishing between the hippocampal subregions was to understand whether AD differentially impacted CA1 and CA3 place cells, the location and size of some tetrode tip marking lesions (see Surgery and histology) made it difficult to distinguish definitively between CA2 and CA3 regions during histological inspection. Thus, data from these tetrodes were combined into one region subsequently referred to as CA2/3.

Quantification of spatial characteristics of spiking data: The firings rates of hippocampal pyramidal neurons often relate closely to the rat's position in an environment (O'Keefe and Dostrovsky, 1971). A main question in the present study was thus whether the spiking activity of CA1 or CA2/3 pyramidal neurons from AD rats would show reduced spatial correlates as compared to neurons from WT rats and whether administration of an M_1 mAChR agonist might ameliorate any possible AD-related reductions. To address this overall question, several spatial measures were calculated for each pyramidal neuron recorded from AD and WT rats for each control and drug session (see below for descriptions of each measure). For each neuron recorded in a session, a spatial firing rate grid was calculated first by partitioning the aerial-view video of the testing environment into 60 by 80 spatial bins of 2.20 cm^2 each. The number of spikes emitted by the neuron while the rat occupied a spatial bin was then divided by the total time the rat spent in that particular bin. Analyses focused on neurons that emitted at least 100 spikes in a session when the rat was running laps and excluded data recorded in the very end of the central stem runway (where rats consumed the small chocolate reward after the completion of each lap), as hippocampal spatial correlates are typically observed during locomotion rather than stationary moments of consummatory behaviors.

The primary measurement of spatial correlates for each neuron's spiking activity was a calculation of a spatial information score (Skaggs et al, 1996), a widely-used metric that reflects the spatial fidelity of the neuron's spiking activity. Specifically, spatial information scores reflect the amount of spatial information emitted by each spike in terms of bits per spike, using the formula:

$$\sum_{i=1}^{N} p_i \left(\frac{R_i}{R}\right) log_2 \left(\frac{R_i}{R}\right),$$

where p_i = probability the rat was at spatial bin *i* (out of N bins), R_i = firing rate at spatial bin *i*, and R = overall firing rate of the place cell (Skaggs et al., 1996).

Pyramidal cells were further characterized as "place cells" if they had at least one area of the environment (place field) in which the firing rate of the unit preferentially increased when the rat was within that place field relative to other locations in the environment. Place field boundaries were determined by the bins in which the firing rates were at least 10% of the maximum in-field firing rate. Note that this calculation does not exclude the possibility that a given unit could have multiple place fields. However, putative place cells with four or more place fields (10 out of the total 1,112 pyramidal units recorded; 0.9%) were excluded from analyses based on the likelihood that these cells were not typical place cells. Place fields with an area of less than 10 bins or for which more than 10% of the in-field spikes would have occurred within the center stem (where rats consumed the food reward after each lap) were excluded from the analyses to minimize the possibility that spurious activity could be labeled as a place field. In addition, place cells were excluded from analyses if the rat did not traverse its place field (or at least one field if a cell exhibited multiple) on at least half of the laps (e.g., place fields for which spiking was visible only when the rat leaned its head to the side of the track).

A second main approach to quantifying the spatial fidelity of place cells was based on the idea that spiking inside a place field represented spatial signal whereas spiking outside a place field represented noise. In particular, a ratio was calculated for each neuron based on the relative proportion of spiking occurring inside versus outside a place field. Overall out-of-field firing rates for each place cell were calculated using all spikes not occurring inside any field while rats were running laps. For each place cell, a proportion of in-field firing was then calculated using the following formula: mean in-field firing rate / (mean in-field firing rate + mean out-of-field firing rate). For place cells with more than one place field, the mean in-field firing rate was based on an average across fields. Spiking activity inside place fields occupying the center of the stem or for which rats traversed on less than half of the laps were excluded from analyses.

Local field potential acquisition and analysis: In addition to the spiking data, local field potentials (LFPs) were recorded from one tetrode in CA1 and one tetrode in CA3 in each session (useable data for CA1 was not available for one AD rat). Tetrodes located in the pyramidal layer (as determined by the presence of pyramidal neuron action potentials) were used for each region. LFPs were recorded continuously at a sampling rate of 1500 Hz and filtered at 1–400 Hz with the NSpike data acquisition system (nspike.sourceforge.net). LFP data were analyzed in MATLAB with a combination of custom scripts and an open source library of functions to calculate power spectra for CA1 and CA3 (Chronux; Bokil et al., 2010). Power was calculated using multi-taper fast fourier transforms (Bokil et al., 2010). To minimize complications that can arise when assuming oscillatory data is stationary (Mitra and Pesaran, 1999), spectral estimates of the LFPs were calculated in time windows of 0.5 seconds. Power estimates of CA1 and CA3 were log10 transformed then multiplied by 10 to convert from bels to decibels, and bias corrected to allow for statistical comparison. The analyses focused on theta (7–9 Hz), slow gamma (30–55 Hz), and fast gamma (65–90 Hz) frequency ranges based on the prominence of these oscillations in the hippocampus (Colgin

et al., 2009) and possible relation to AD-related hippocampal dysfunction (e.g. Mably et al., 2017). For the slow gamma and fast gamma frequency bands, we used 5 tapers so that the spectral estimates for each frequency was averaged across +/− 6 Hz. For the theta frequency band, we used 1 taper so that spectral estimates were averaged across +/− 2 Hz. The relationship between time window (T), frequency range half bandwidth (W) and number of tapers (K) is specified by the formula: K = 2TW – 1 (Mitra and Pesaran, 1999).

LFP power spectra as rats were completing laps on the circle track were analyzed as a function of the rat's speed of locomotion because both theta and gamma oscillations have been shown to correlate with locomotion speed (Ahmed and Mehta, 2012). Locomotion speeds were calculated by the frame-to-frame change in the x and y coordinates of the rat within a session and were split into three bins (stationary = 1–12 cm/sec, slower running = 13–25 cm/sec, faster running = 26–62 cm/sec). Power was calculated from the data within each running bin separately and then averaged. The number of 0.5-second sweeps in each run bin for different rats and different run bins was variable, and a low number of sweeps can upwardly bias spectral estimates. Thus, we found the minimum number of 0.5-second sweeps for each rat over all sessions and run bins. Then for each run bin within a session for a given rat, we subsampled from the total sweeps in that run bin 500 different times, and calculated spectral estimates using that rat's minimum sweep number of randomly scrambled sweeps. The final power for one run bin of one session of one rat reflects the mean across all 500 subsamples. This approach minimized the possibility that differing locomotion speeds between sessions would have determined spectral results. Gamma power is shown from data collected when rats were stationary, and theta power is shown from data collected when rats were not stationary.

Spike-phase modulation acquisition and analysis: In order to evaluate the depth of spike modulation in CA1 and CA2/3 place cells relative to CA1 theta, CA1 theta phase was obtained using a waveform-based method (see Trimper et al., 2014) and the phase of theta for each spike of CA1 and CA2/3 place cells was calculated using an open-source circular statistics toolbox for MATLAB (Berens, 2009) to obtain the mean resultant vector length for each place cell.

Adjusting data for age: The age at testing varied across rats (range: 12–20 months) in part due to data collection bottlenecks inherent to single-unit *in vivo* electrophysiology. In order to account for the possibility that hippocampal activity was influenced by age in both AD and WT rats, age-adjusted values for each place cell metric (spatial information scores, in-field firing rates, proportion of in-field firing), LFP power, and spike-field mean resultant length were calculated by first regressing each variable with rat age in months (including data from both AD and WT rats in one model) and by then adding the residuals to the original grand mean. This approach is similar to including age as a covariate in each ANOVA and was taken to minimize the possibility that the slightly older age of the AD rats (mean age = 17.0 mo vs. 15.5 mo for WT) did not disadvantage their data. As one example of the approach, a linear regression of spatial information scores by age revealed a statistically significant effect of age ($F[1,1100]=66.19$, $p<0.001$; $R^2 = 0.06$), although the effect was modest (β for age = −0.095; each month of age corresponding to a 0.095 lower

spatial information score on average). Figure 3 shows these spatial information scores plotted for each pyramidal neuron by the rat's age before and after adjusting for age. Although the data are similar after adjusting for age, the adjustment was an important analysis step. All plotting and statistical analyses were conducted with age-adjusted values unless noted otherwise.

Results

Table 1 shows the number of CA1 and CA2/3 pyramidal cells and place cells recorded from 4 WT and 7 AD rats for the control and drug conditions. Figure 4 shows example CA1 and CA2/3 place field plots for WT and AD rats recorded during the control condition. The examples depict the general finding across conditions that CA2/3 place cells from WT rats and CA1 place cells from both WT and AD showed well-circumscribed spatial receptive fields in which firing rates were increased relative to the low baseline rates observed when rats occupied locations outside a neuron's receptive field. That is, many hippocampal pyramidal neurons—including those in region CA1 for the AD rats—were place cells that showed what appeared to be good spatial fidelity. In comparison, CA2/3 place cells for AD rats tended to show poor spatial fidelity. Accordingly, we used a variety of quantitative metrics to compare the spatial fidelity of place cells from AD and WT rats and to test if the M_1-selective mAChR agonist VU0364572 increased the spatial fidelity of place cells in AD rats.

AD and WT rats had similar locomotion speeds across control and drug conditions—Firing rates of hippocampal neurons often correlate with a rat's speed of locomotion (e.g. Huxter et al., 2003), and thus an important initial question was whether AD rats moved faster or slower than WT rats or whether locomotion speed for either group was influenced by drug administration. Accordingly, we calculated the age-adjusted average locomotion speed for every session for each rat. The mean locomotion speed (cm/s) was similar between AD and WT rats and across drug conditions ($M \pm SEM$: WT = 20.90 ± 3.0, 20.47 ± 2.3, 20.58 ± 1.9 for control, 10 mg/kg VU0364572, and 30 mg/kg VU0354572; AD = 20.55 ± 1.7, 22.48 ± 1.9, 22.01 ± 2.1 for control, 10 mg/kg VU0364572, and 30 mg/kg VU0354572). A two-way (2×3; genotype by drug condition) ANOVA for locomotion speeds found no significant differences in run speed between genotypes, across drug conditions, or a genotype by drug interaction (all ps > 0.10). In addition, one-way ANOVAs for speeds across drug conditions were conducted separately for AD rats ($F[2,18]=0.24$, p=0.79, $\eta_p^2=0.03$) and WT rats ($F[2,9]=0.01$, p=0.99, $\eta_p^2=0.00$) and also revealed no significant effect of drug administration. Thus, it is unlikely that any differences in the subsequent analyses of neural data were the indirect result of differences in locomotion speed.

Hippocampal CA2/3 but not CA1 place cells of AD rats showed impaired spatial fidelity—A main question of interest was whether place cell activity might differ between AD and WT rats or across drug conditions. Many studies have found differences between CA1 and CA3 place cell characteristics (Leutgeb and Leutgeb, 2007; Mizuseki et al., 2012) and subregional differences in hippocampal function in aging and AD (e.g. Bakker et al., 2012; Thomé et al., 2015). Thus, we assessed place cell activity separately for CA1 and CA2/3 pyramidal neurons (see Materials and Methods). In particular, variables were

analyzed with three-way (2×2×3) ANOVAs that distinguished CA1 and CA2/3 activity (hippocampal region by genotype by drug condition). In addition, to ask more specifically if place cell activity differed between AD and WT rats with or without drug administration, two-way (hippocampal region by genotype) ANOVAs were conducted separately for the control and drug conditions. Supplementary Tables 1 to 9 show full ANOVA tables for each of the analyses described below.

Figure 5 (panel A) shows average place cell fidelity for WT and AD rats calculated as age-adjusted spatial information scores, a widely-used metric for quantifying spatial correlates of spiking activity (see Materials and Methods). The results were calculated separately for CA1 and CA2/3 pyramidal neurons meeting the criterion for place cells and were plotted separately for the control and drug sessions. An overall three-way ANOVA (genotype by region by drug condition) identified an effect of genotype ($F[1,1100]=12.69$, $p<0.001$) and hippocampal region ($F[1,1100]= 22.31$, $p<0.001$), indicating that in general place cells in WT rats had generally higher spatial information scores relative to place cells in AD rats and that CA1 place cells had generally higher spatial information scores relative to CA2/3 place cells (see Supplementary Table 1 for detailed statistics). However, the difference between spatial information scores for AD and WT rats depended on whether the place cells were recorded in CA1 or CA2/3 (genotype x region interaction: $F[1,1100]=20.04$, $p<0.001$). Indeed, the CA1 spatial information scores for AD rats were similar to those of WT rats, but the CA2/3 spatial information scores for AD rats were markedly lower than those of WT rats. Supplementary Figure 1 replots the AD data as a normalized (Z scored) difference from the WT data and highlights the CA2/3-specific impairment for the AD rats. There was no significant effect of drug condition ($F[2,1100]=0.94$, $p=0.39$). To ask more specifically if the pattern of impaired CA2/3 and spared CA1 place cell fidelity in AD rats would be apparent with or without drug administration, two-way (hippocampal region by genotype) ANOVAs were conducted separately for the control and drug conditions (see Supplementary Table 1). The interaction between genotype and hippocampal region was statistically significant for the control condition ($F[1,374]=4.18$, $p<0.05$), the 10 mg/kg M_1 agonist condition ($F[1,365]=8.58$, $p<0.01$), and the 30 mg/kg M_1 agonist condition ($F[1,361]=7.57$, $p<0.01$). Thus, the results indicated that AD rats showed reduced spatial fidelity selectively for CA2/3 place cells and that this impairment was similar across control and drug conditions.

One potential concern with this analysis of spatial information scores was the possibility that our criterion for labeling a neuron as a place cell (see Materials and Methods) could have influenced the results. For example, any reduced spatial fidelity for place cells in AD rats could have decreased the likelihood that these neurons would be labeled as place cells. If so, the exclusion from the analyses of the poorest place cells for the AD rats could have attenuated differences between AD and WT rats. In order to address this possibility, the spatial information scores for all pyramidal neurons were calculated regardless of whether the neuron was determined to be a place cell. The pattern of results from spatial information scores calculated from all pyramidal neurons was similar to the pattern obtained with only those pyramidal neurons judged to be place cells. Specifically, the CA1 spatial information scores for AD rats were similar to those of WT rats, but the CA2/3 spatial information scores for AD rats were markedly lower than those of WT rats ($M \pm SEM$: CA1 WT = 2.32 ± 0.09, 2.28 ± 0.08, 2.37 ± 0.09 for control, 10 mg/kg VU0364572, and 30 mg/kg

VU0364572; CA1 AD = 2.23 ±0.13, 2.45 ± 0.18, 2.51 ± 0.20 for control, 10 mg/kg VU0364572, and 30 mg/kg VU0364572; CA2/3 WT = 2.21 ± 0.10, 2.28 ± 0.10, 2.34 ± 0.10 for control, 10 mg/kg VU0364572, and 30 mg/kg VU0364572; CA2/3 AD = 1.75 ±0.07, 1.77 ±0.07, 1.78 ± 0.07 for control, 10 mg/kg VU0364572, and 30 mg/kg VU0364572). An overall three-way ANOVA (genotype by region by drug condition) again identified a significant genotype by hippocampal region interaction (F[2,1367]=4.39, p<0.05). Thus, the selective reduction in spatial fidelity for CA2/3 place cells in AD rats relative to WT rats applied to all pyramidal neurons and did not depend on our criterion for identifying place cells.

A second question was whether the place cells from the CA2/3 region in AD rats would show reduced spatial information scores relative to WT rats if pyramidal neurons in or near the CA2 region were excluded from the analysis. Similar to the pattern of results from spatial information scores including units recorded from tetrodes in CA2 or on the CA2/3 border, CA3 spatial information scores for AD rats were markedly lower than those of WT rats (M ± SEM: CA3 WT = 2.33 ± 0.14, 2.35 ± 0.14, 2.47 ± 0.14 for control, 10 mg/kg VU0364572, and 30 mg/kg VU0364572; CA3 AD = 1.53 ±0.12, 1.85 ±0.12, 1.90 ± 0.12 for control, 10 mg/kg VU0364572, and 30 mg/kg VU0364572). An overall three-way ANOVA (genotype by region by drug condition) again identified a significant genotype by hippocampal region interaction (F[2,798]=16.04, p<0.001).

M_1 agonism influenced AD and WT hippocampal place cell in-field firing rates but not ratios of in to out-of-field firing rates—We next asked if more direct measures of spiking activity might further inform possible differences between AD and WT rats or reveal the influence of drug administration. In particular, we calculated for each place cell the average firing rate inside versus outside a cell's place field(s) based on the idea that in-field spiking might represent a signal regarding the rat's location whereas out-of-field spiking might represent noise. Figure 5 (panel B) shows for AD and WT rats the mean in-field firing rates for CA1 and CA2/3 place cells in the control and drug conditions (see also Supplementary Figure 1B for plots of the AD data normalized to WT data). In general, for both CA1 and CA2/3 place cells, oral administration of the M_1-selective mAChR agonist VU0364572 increased in-field firing rates for WT rats but decreased in-field firing rates for AD rats. An overall three-way ANOVA (genotype by region by drug condition) for in-field firing rates identified significant genotype by drug interaction (F[2,1100]=3.49, p<0.05; see Supplementary Table 2). Additional two-way (hippocampal region by genotype) ANOVAs were conducted separately for the control and drug conditions (see Supplementary Table 2). In contrast to the pattern of results from spatial information scores, the in-field firing rates of CA1 and CA2/3 place cells did not significantly differ between AD and WT rats in the control condition (p=0.33) but diverged with oral administration of the M_1-selective mAChR agonist VU0364572, particularly at the higher 30 mg/kg dose (p <0.05).

We next sought to address the discrepancy between the pattern of results from in-field firing rates and spatial information scores by asking if a proportion of in-field (signal) and out-of-field (noise) firing rates might correspond better to a place cell's spatial fidelity rather than absolute in-field firing rates. Figure 5 (panel C) shows this proportion of in-field firing (calculated as: mean in-field / [mean in-field + mean out-of-field]) for CA1 and CA2/3 place

cells for AD and WT rats across control and drug conditions (see also Supplementary Figure 1C for plots of the AD data normalized to WT data). The pattern of results closely resembled those observed with spatial information scores. Specifically, the CA1 ratios for AD rats were very similar to those of WT rats, the CA2/3 ratios for AD rats were markedly lower than those of WT rats, and there was no overall apparent effect of drug condition. An overall three-way ANOVA (genotype by region by drug condition) revealed a genotype by hippocampal region interaction ($F[1,1100]=6.26$, $p<0.05$), an effect of genotype ($F[1,1100]=12.56$, $p<0.001$), an effect of hippocampal region ($F[1,1100]=19.97$, $p<0.001$), but no effect of drug condition ($F[2,1100]=0.52$, $p=0.60$), all of which were similar to the findings for spatial information scores (see Supplementary Tables 1 and 3). When the in-field proportions for the control condition were evaluated separately, a two-way (genotype by region) ANOVA revealed an effect of genotype ($F[1,374]=5.35$, $p<0.05$) and region ($F[1,374]=7.10$, $p<0.01$) and an interaction that approached statistical significance ($F[1,374]=3.25$, $p=0.07$). These results indicate that although administration of the M_1-selective mAChR agonist VU0364572 significantly influenced in-field firing rates of place cells, these effects of M_1 agonism were balanced by the effects on out-of-field firing rates such that proportions of in-field firing rates were similar to the control condition. Just as with the spatial information scores, the proportion of in-field firing was impaired in AD CA2/3 place cells and there was no evidence that M_1 agonism improved the proportion of in-field firing rate.

CA2/3 but not CA1 place fields were larger in AD rats as compared to WT rats—We next asked if the reduced spatial fidelity of CA2/3 place cells in AD rats relative to WT rats was related to larger place fields and/or an increased number of place fields per cell. Table 2 shows for CA1 and CA2/3 place cells the mean place field area and mean number of place fields per unit for WT and AD rats across the control and drug conditions. For place field area, an overall three-way ANOVA (genotype by region by drug condition) identified an effect of genotype ($F[1,1100]=7.46$, $p<0.01$; see Supplementary Table 4). However, similar to the findings for spatial information scores and proportion of in-field firing, the difference in place field size between AD and WT rats depended on whether the cells were recorded in CA1 or CA2/3 (genotype by region interaction: $F[1,1100]=5.25$, $p<0.05$). There was no statistically significant effect of the M_1-selective mAChR agonist VU0364572 ($F[2,1100]=0.38$; $p=0.69$). For the control condition, CA1 place fields were similar in size between AD and WT rats but CA2/3 place fields were larger in AD rats as compared to WT rats (two-way ANOVA for the control condition; genotype by region interaction: $F[1,374]=3.76$, $p=0.05$; see Supplementary Table 4). The mean number of place fields per CA1 and CA2/3 place cell was close to 1 across drug conditions for AD and WT rats (range = 1.11 to 1.32). An overall three-way ANOVA (genotype by region by drug condition) identified no significant overall effects of genotype, region, or drug condition (all ps > 0.100), yet did result in a significant interaction between genotype and drug condition ($F[1,1100]=4.77$, $p<0.01$; see Supplementary Table 5). Thus, place field size paralleled spatial information scores in identifying dysfunction in AD rats specific to CA2/3, whereas the number of fields per place cell paralleled absolute in-field rates in identifying divergent effects of M_1 agonism on place cell activity in AD versus WT rats.

M_1 agonism influenced theta modulation of spiking differently for AD and WT place cells—Neuronal oscillations are important to normal place cell function, and thus we next asked whether theta or gamma oscillations differed between AD and WT rats or were influenced by administration of the M_1-selective mAChR agonist, VU0364572. Table 3 shows the mean power (dB) of theta (7–9 Hz), slow gamma (30–55 Hz) and fast gamma (65–90 Hz) oscillations in CA1 and CA3 pyramidal cell layers for AD (n=5) and WT (n=4) rats with LFP data from both hippocampal regions across the control and drug conditions. The mean CA1 and CA3 power for theta, slow gamma, and fast gamma was similar for AD and WT rats and was not significantly influenced by drug administration (three-way ANOVAs: all ps > 0.1; see Supplementary Tables 6, 7, and 8). One important consideration for these results is that oscillatory power was obtained from tetrodes in the pyramidal layers of CA1 and CA3 and that the results might have differed, particularly for the slow gamma and fast gamma ranges, if oscillatory power had been obtained from dendritic layers such as radiatum or lacunosum-moleculare (e.g., Schomberg et al., 2014; Lasztóczi, & Klausberger, 2016).

The periodicity of place cell spiking is typically strongly modulated by the phase of the hippocampal theta rhythm (O'Keefe and Recce, 1993), and thus we also asked if the extent of theta modulation of spiking might differ between AD and WT rats. The depth of theta modulation for each place cell was calculated as the length of the mean resultant vector determined by the theta phase of each spike (see Material and Methods: number of place cells = 485 in CA1 and 425 in CA2/3, across 4 WT and 6 AD rats). Figure 5 (panel D) shows the mean resultant lengths for CA1 and CA2/3 place cells from AD and WT rats across control and drug conditions (see also Supplementary Figure 1D for plots of the AD data normalized to WT data). An overall three-way ANOVA (genotype by region by drug condition) identified an effect of region ($F[1,898]=39.87$, $p<0.001$), reflecting a general tendency of CA2/3 place cell spiking to be more strongly modulated by theta relative to CA1 (see Supplementary Table 9). The results also revealed an effect of genotype ($F[1,898]=4.17$, $p<0.05$) and an interaction between genotype and drug condition ($F[2,898]=4.37$, $p<0.05$). The interaction reflected the trend for CA1 and CA2/3 mean resultant lengths to be similar for AD and WT rats for the control and 10 mg/kg drug conditions but dissimilar for the 30 mg/kg drug condition. Follow-up two-way ANOVAs (genotype by region) for each drug condition confirmed that the mean resultant lengths were significantly lower for AD versus WT rats in the 30 mg/kg M_1 agonist condition ($F[1,296]=11.62$, $p<0.01$) but not in the control or 10 mg/kg M_1 agonist conditions (ps > 0.10; see Supplementary Table 9). These results resemble the trends observed for CA1 and CA2/3 in-field firing rates and number of fields per cell insofar as administration of the M_1-selective mAChR agonist VU0364572 led to differences between WT and AD rats that did not exist in the control condition.

Impact of adjusting data for rat age—All of the results for Experiment 2 reported above were adjusted to take account of rats' age (see "*Adjusting data for age*" in Materials and Methods). This procedure was an important step taken to minimize the possibility that the AD rats' slightly higher age (mean = 17.0 mo) as compared to the age of WT rats (mean = 15.5 mo) did not lead to spuriously decreased estimates of hippocampal activity in the AD rats. Nevertheless, we also recalculated all of the results without accounting for rats' age and

observed largely similar results. Supplementary Figure 2 (panels A-D) replots the data from Figure 5 without adjusting for age. In addition, Supplementary Tables 10 to 18 show ANOVA tables that parallel those in Supplementary Tables 1 to 9 except that Supplementary Tables 10 to 18 report results when data were not adjusted for rats' age. The pattern of results between AD and WT rats and across drug conditions are similar whether or not the data were adjusted for age. For example, regardless of age-adjustment, spatial information scores across drug conditions for CA2/3 place cells were lower for AD rats as compared to WT rats, whereas for CA1 place cells were similar between groups of rats (see Figure 5A, Supplementary Figure 2A, and Supplementary Tables 1 and 10). Thus, adjusting for age was an important step in the analyses to ensure that lower AD scores were not attributable to a slightly older age, but the age adjustment did not introduce substantial differences in the pattern of results.

General Discussion

The results of Experiment 1 indicated that AD rats showed impaired spatial memory relative to WT rats by 9 to 12 months of age. The results of Experiment 2 indicated that, to the extent that this memory impairment was related to dysfunction in the hippocampus, it was more attributable to dysfunction in regions CA2 and CA3 rather than CA1. Specifically, we investigated how hippocampal place cell function differed between AD and WT rats who were at least 12 months of age (but no older than 20 months) and found that spatial fidelity of hippocampal place cells was impaired in AD rats for CA2/3 pyramidal neurons but not CA1 pyramidal neurons. Other measures of hippocampal function, such as the power of theta and gamma oscillations in the CA1 and CA3 LFPs, were similar between AD and WT rats, suggesting that the spatial memory impairment was more closely related to place cell dysfunction as compared to these other measures. The results also indicated that oral administration of an M_1–specific mAChR agonist (VU0364572) influenced firing rates and depth of spike theta phase modulation of hippocampal place cells in both AD and WT rats but did not improve the reduced spatial fidelity of CA2/3 place cells in AD rats. These results are considered in more detail below.

Specificity of hippocampal place cell dysfunction in a rat model of AD

By 9 to 12 months of age, the AD rats showed impaired spatial memory performance that was no better than one would expect by chance (Fig. 2). Despite this marked memory impairment, no differences between AD and WT rats aged 12–20 months were observed in any measure of CA1 place cell activity or local field potentials in the absence of drug administration (Fig. 5; Tables 2 and 3). In contrast, CA2/3 place cells in AD rats showed reduced spatial information scores (Fig. 5), lower proportions of in-field firing (Fig. 5), and increased place field size (Table 2) relative to CA2/3 place cells in WT rats in the control condition. The type of spatial memory assessed by the object-in-location memory task is known to depend on the hippocampus (Barker and Warburton, 2011), and thus one main implication is that it was possible that the spatial memory impairment exhibited by AD rats in the present study was due at least in part to the reduced spatial fidelity of place cells in hippocampal regions CA2 and/or CA3. An important caveat to this interpretation is that the reduced spatial fidelity of CA2/3 place cells in Experiment 2 were observed outside the

context of an explicit memory task and cannot be causally linked to the spatial memory deficits in Experiment 1. A related second point is that CA1 place cell function was spared in AD rats aged 12 to 20 months. A prior study that extensively characterized the neuropathology of the AD rats (Cohen et al., 2013) found that, by 16 months of age (close to the mean age of rats in the present study at the time of recording), AD rats showed throughout the hippocampus and neocortex significantly increased markers of Aβ deposits, tau pathology, and cell loss relative to WT rats. Thus, the normal CA1 place cell spatial fidelity observed in 12–20 month-old AD rats contrasts with their memory impairments, CA2/3 place cell dysfunction, and neuropathology. The contrast is striking in part because CA3 pyramidal neurons are one of the most prominent sources of direct input to CA1 pyramidal neurons (Witter et al., 2000).

One potential explanation for the spared CA1 and impaired CA2/3 place cell function could be due to differing inputs to these regions from the entorhinal cortex, the main source of cortical inputs to the hippocampus (Lavenex and Amaral, 2000; Witter et al., 2000). In particular, CA1 receives direct projections from layer III of entorhinal cortex, whereas CA2 and CA3 both receive direct projections from layer II of entorhinal cortex (Llorens-Martin et al., 2014; Steward and Scoville, 1976). In humans, layer II of the lateral entorhinal cortex is one of the first brain regions to be impacted by tau pathology and shows disproportional neuronal loss (Gomez-Isla et al., 1996; Llorens-Martin et al., 2014; Yassa, 2014). Thus, the intact spatial fidelity of CA1 place cells of AD rats suggests that the dysfunctional input it is receiving from CA3 may be offset by intact inputs from layer III of the entorhinal cortex. This possibility is supported by previous studies that showed CA1 place cells were able to form normal place fields without input from CA3, but not without input from layer III of the entorhinal cortex (Brun et al., 2002; Brun et al., 2008). Nevertheless, future studies would be needed to determine with more certainty whether differential pathology in layers II versus III of the entorhinal cortex would relate to differences between CA1 and CA2/3 place cell spatial fidelity in AD rats. Indeed, an alternate possibility is that entorhinal cortex inputs to both CA1 and CA2/3 are intact at 12–20 months of age in AD rats and that the CA2/3 dysfunction relates more closely to intra-hippocampal pathology at this age (e.g., in upstream dentate gyrus or CA3 itself).

An important remaining question is how CA2/3 dysfunction in AD rats related to the memory impairment and disease progression. A straightforward interpretation is that pathological molecular processes related to AD (e.g., amyloid and/or tau pathology) led to neuronal dysfunction in CA2/3, which impaired AD rats' memory. It is also possible that the neuronal dysfunction in CA2/3 exacerbated the pathological progression. For example, prior studies have found that exciting hippocampal neurons of AD mice increases the secretion of soluble Aβ (Noebels, 2011). Soluble Aβ in turn can increase cellular excitability and can be toxic to cells (Findeis, 2007; Noebels, 2011; Palop et al., 2007). The present data from extracellular recordings cannot speak directly to membrane dynamics, but one idea to pursue in future research is the possibility that dysfunctional activity of CA2/3 pyramidal cells early in AD could accelerate the disease progression in the hippocampus. Recording hippocampus activity of AD rats at 6 months of age or younger, well before amyloid or tau pathology begins to increase, would help uncover if CA2/3 place cell dysfunction precedes and perhaps plays a causal role in the pathological progression of AD.

Hippocampal place cell spatial fidelity in relation to other rodent models of AD

The current results added to prior findings from studies in transgenic mouse models of AD showing evidence of general hippocampal dysfunction (Morrissette et al., 2009), including reduced fidelity and increased size of hippocampal CA1 place cells, reduced LFP power in the theta or gamma range, and reduced depth of theta phase modulation of spikes in AD relative to WT mice (Booth et al., 2016; Cacucci et al., 2008; Cayzac et al., 2015; Cheng and Ji, 2013; Mably et al., 2017; Rubio et al., 2012; Zhao et al., 2014). The current study also found hippocampal dysfunction in AD rats, but in contrast to these prior studies in mice, observed deficits only in CA2/3 place cells. The prior mouse studies did not report data for CA2 or CA3 pyramidal neurons, but in the present study CA1 place cells in 12–20 month-old AD rats showed good levels of spatial fidelity. One possibility for the discrepancy with respect to CA1 place cell fidelity between the current results and findings with AD mouse models is that the somewhat slower time course of disease progression in the AD rat model (Cohen et al., 2013) relative to some mouse AD models (see Hall and Roberson, 2012) created an opportunity to detect changes that occur earlier in the disease, before the pathological progression could cause ubiquitous dysfunction in brain memory circuits. If so, recordings from AD mice in both CA1 and CA3 regions at a very early stage of the disease would also be expected to show dysfunctional CA2/3 place cells prior to the onset of dysfunction in CA1 place cells.

In addition to differing age-related trajectories of disease progression between the Tg-F344 AD rat model and many mouse AD models, there are also several important genetic and pathological differences between rodent models of AD. The transgenic rat model of AD used in the current study expresses two genetic mutations (APPSwe and PS1ΔE9) that are found in humans with familial AD and shows many of the same pathological features that are seen in human AD, including age-dependent robust tau pathology, markers of neuroinflammation, and cell death (Cohen et al., 2013). Rats (Rattus novegicus) share six isoforms of tau protein with humans, whereas mice (Mus musculus) share three isoforms of tau with humans (McMillan et al., 2008; Hanes et al., 2009). As a result, many of the mouse models of AD used to investigate hippocampal place cells have utilized tau mutations that are not found in humans with AD in order to induce tau pathology (e.g. Booth et al., 2016; Cheng & Ji, 2013; Mably et al., 2017). It is unclear the extent to which these tau-related genetic differences between mice and rats can explain the differences in CA1 place cell findings between the current study in rat and past studies in mice, but the question will be worth pursuing in future studies aimed at understanding human AD.

Administration of M_1 agonist influenced place cell spiking but not place cell spatial fidelity

Recent experimental evidence indicated that increasing M_1 muscarinic acetylcholine receptor activity reduced AD pathology and cognitive impairment in AD mice (Lebois et al., 2017) and increased spatial correlates in young WT rats (Lebois et al., 2016). Thus, a second main question was whether oral administration of an M_1-speicifc mAChR agonist (VU0364572) would ameliorate any AD-related hippocampal dysfunction. Although the M_1 agonist did not appreciably change any of the metrics related to spatial fidelity in which AD CA2/3 place cells were significantly impaired relative to WT CA2/3 place cells (spatial information scores, proportion of in-field firing, and place field area), the M_1 agonist did

influence in-field firing rates and spike-phase modulation. Specifically, there were no differences between AD and WT in the control condition for in-field firing rates and spike-phase modulation, yet differences emerged following administration of the M_1 agonist. For example, the M_1 agonist numerically increased the in-field firing rates of WT place cells but numerically decreased the in-field firing rates of AD place cells, suggesting that the impact of the drug depended on the functional state of the brain prior to administration. The effects of the M_1 agonist on in-field firing rates were not reflected in spatial information scores, perhaps because the effects on in-field firing rates were offset by effects on out-of-field firing rates such that the proportion of in-field firing was similar across drug conditions. VU0364572 was chosen for the present study in part because it is a direct agonist and can therefore activate the M_1 muscarinic receptor even if endogenous levels of acetylcholine were reduced. Nevertheless, one consideration for future studies is that chronic dosing of an M_1 mAChR agonist such as VU0364572 may be needed to impact AD progression (see Lebois et al., 2017). Another consideration is the possibility that an M_1 positive allosteric modulator, which would augment the activity of endogenous and phasically-released acetylcholine at the M_1 receptor, might benefit AD-related hippocampal dysfunction in ways that the M_1 agonist VU0364572 did not. In any case, the M_1 agonist did influence spiking activity in the hippocampus, and the difference between genotypes, subregions, and various metrics of hippocampal function points to the usefulness of using *in vivo* electrophysiology to understand effects of potential drug therapies on brain function.

Conclusion

The slower-paced accumulation of AD-pathology in the TgF344 AD rat model (frank pathology by 16 months of age; Cohen et al., 2013) may be particularly useful for investigating early impairments in cellular and neural network dysfunction that occur before Aβ plaques or tau pathology has spread extensively throughout the brain. For example, future studies could examine hippocampal spatial fidelity in AD rats as early as 6 months of age, when Aβ plaques have not formed but soluble oligomeric fibrillar Aβ and markers of inflammation are already elevated above age-matched WT controls (Cohen et al., 2013). Moreover, recording studies in AD rats can benefit from decades of data on place cell function in healthy rat brains. Indeed, the current study highlighted the possibility that network dysfunction relatively restricted to the CA2/3 regions of the hippocampus may occur in AD before the peak of molecular and protein abnormalities, widespread brain dysfunction, and irreversible cell death occurs. Given that age is a major risk factor of the majority of “sporadic” AD cases in humans that are not linked to specific genetic mutations (Kukull et al., 2002), future studies should investigate how age-related dysfunction interacts with dysfunction related to AD pathology. The results also pointed to the potential for using techniques like *in vivo* electrophysiology in AD rats to understand how function and dysfunction relate to neuropathology and how potential drug therapies might influence dynamic brain circuits.

Supplementary Material

Refer to Web version on PubMed Central for supplementary material.

Acknowledgments

Grants: National Institute of Health - NIA-R21AG042730

We thank Megan Airey, Jason Schroeder, Sophia Zhang, and Jay Li for their assistance and the Vanderbilt Center for Neuroscience Drug Discovery for providing VU0364572. This work was supported by NIH grant NIAR21AG042730.

References

Ahmed OJ, Mehta MR. Running speed alters the frequency of hippocampal gamma oscillations. The Journal of Neuroscience. 2012; 32(21):7373–7383. DOI: 10.1523/JNEUROSCI.5110-11.201 [PubMed: 22623683]

Anand P, Singh B. A review on cholinesterase inhibitors for Alzheimer's disease. Archives of Pharmacal Research. 2013; 36(4):375–399. DOI: 10.1007/s12272-013-0036-3 [PubMed: 23435942]

Bakker A, Krauss GL, Albert MS, Speck CL, Jones LR, Stark CE, … Gallagher M. Reduction of hippocampal hyperactivity improves cognition in amnestic mild cognitive impairment. Neuron. 2012; 74(3):467–474. DOI: 10.1016/j.neuron.2012.03.023 [PubMed: 22578498]

Barker GRI, Warburton EC. When is the hippocampus involved in recognition memory? The Journal of Neuroscience. 2011; 31(29):10721–10731. DOI: 10.1523/JNEUROSCI.6413-10.2011 [PubMed: 21775615]

Bartus RT, Dean RL, Beer B, Lippa AS. The cholinergic hypothesis of geriatric memory dysfunction. Science. 1982; 217(4558):408–417. DOI: 10.1126/science.7046051 [PubMed: 7046051]

Berens P. CircStat: A MATLAB toolbox for circular statistics. Journal of Statistical Software. 2009; 31(10):1–21.

Bokil H, Andrews P, Kulkami JE, Mehta S, Mitra PP. Chronux: A platform for analyzing neural signals. Journal of Neuroscience Methods. 2010; 192(1):146–151. DOI: 10.1016/j.neumeth.2010.06.020 [PubMed: 20637804]

Booth CA, Witton J, Nowacki J, Tsaneva-Atanasova K, Jones MW, Randall AD, Brown JT. Altered intrinsic pyramidal neuron properties and pathway-specific synaptic dysfunction underlie aberrant hippocampal network function in a mouse model of tauopathy. Journal of Neuroscience. 2016; 36(2):350–363. DOI: 10.1523/JNEUROSCI.2151-15.2016 [PubMed: 26758828]

Braak H, Braak E. Staging of Alzheimer's disease-related neurofibrillary changes. Neurobiology of Aging. 1995; 16(3):271–278. DOI: 10.1016/0197-4580(95)00021-6 [PubMed: 7566337]

Brun VH, Leutgeb S, Wu HQ, Schwarcz R, Witter MP, Moser EI, Moser MB. Impaired spatial representation in CA1 after lesion of direct input from entorhinal cortex. Neuron. 2008; 57(2):290–302. DOI: 10.1016/j.neuron.2007.11.034 [PubMed: 18215625]

Brun VH, Otnæss MK, Molden S, Steffenach HA, Witter MP, Moser MB, Moser EI. Place cells and place recognition maintained by direct entorhinal-hippocampal circuitry. Science. 2002; 296(5576):2243–2246. [PubMed: 12077421]

Bymaster FP, Carter PA, Yamada M, Gomeza J, Wess J, Hamilton SE, … Felder C. Role of specific muscarinic receptor subtypes in cholinergic parasympathomimetic responses, *in vivo* phosphoinositide hydrolysis, and pilocarpine-induced seizure activity. European Journal of Neuroscience. 2003; 17(7):1403–1410. DOI: 10.1046/j.1460-9568.2003.02588.x [PubMed: 12713643]

Cacucci F, Yi M, Wills TJ, Chapman P, O'Keefe J. Place cell firing correlates with memory deficits and amyloid plaque burden in Tg2576 Alzheimer mouse model. Proceedings of the National Academy of Sciences. 2008; 105(22):7863–7868. DOI: 10.1073/pnas.0802908105

Cayzac S, Mons N, Ginguay A, Allinquant B, Jeantet Y, Cho YH. Altered hippocampal information coding and network synchrony in APP-PS1 mice. Neurobiology of Aging. 2015; 36(12):3200–3213. DOI: 10.1016/j.neurobiolaging.2015.08.023 [PubMed: 26391642]

Cheng J, Ji D. Rigid firing sequences undermine spatial memory codes in a neurodegenerative mouse model. Elife. 2013; 2:e00647.doi: 10.7554/eLife.00647 [PubMed: 23805379]

Chhatwal JP, Sperling RA. Functional MRI of mnemonic networks across the spectrum of normal aging, mild cognitive impairment, and Alzheimer's disease. Journal of Alzheimer's Disease. 2012; 31(S3):S155–S167. DOI: 10.3233/JAD-2012-120730

Clark RE, Squire LR. An animal model of recognition memory and medial temporal lobe amnesia: History and current issues. Neuropsychologia. 2010; 48(8):2234–2244. DOI: 10.1016/j.neuropsychologia.2010.02.004 [PubMed: 20144894]

Cohen RM, Rezai-Zadeh K, Weitz TM, Rentsendorj A, Gate D, Spivak I, … Town T. A transgenic Alzheimer rat with plaques, tau pathology, behavioral impairment, oligomeric aβ, and frank neuronal loss. The Journal of Neuroscience. 2013; 33(15):6245–6256. DOI: 10.1523/JNEUROSCI.3672-12.2013 [PubMed: 23575824]

Colgin LL, Denninger T, Fyhn M, Hafting T, Bonnevie T, Jensen O, … Moser EI. Frequency of gamma oscillations routes flow of information in the hippocampus. Nature. 2009; 462(7271):353–357. DOI: 10.1038/nature08573 [PubMed: 19924214]

Conn PJ, Christopoulos A, Lindsley CW. Allosteric modulators of GPCRs: A novel approach for the treatment of CNS disorders. Nature Reviews Drug Discovery. 2009; 8(1):41–54. DOI: 10.1038/nrd2760 [PubMed: 19116626]

DeKosky ST, Scheff SW. Synapse loss in frontal cortex biopsies in Alzheimer's disease: Correlation with cognitive severity. Annals of Neurology. 1990; 27(5):457–64. [PubMed: 2360787]

Dickson DW, Crystal HA, Bevona C, Honer W, Vincent I, Davies P. Correlations of synaptic and pathological markers with cognition of the elderly. Neurobiology of Aging. 1995; 16(3):285–298. DOI: 10.1016/0197-4580(95)00013-5 [PubMed: 7566338]

Digby GJ, Noetzel MJ, Bubser M, Utley TJ, Walker AG, Byun NE, … Conn PJ. Novel allosteric agonists of M1 muscarinic acetylcholine receptors induce brain region-specific responses that correspond with behavioral effects in animal models. The Journal of Neuroscience. 2012; 32(25):8532–8544. DOI: 10.1523/JNEUROSCI.0337-12.2012 [PubMed: 22723693]

Ennaceur A, Delacour J. A new one-trial test for neurobiological studies of memory in rats. 1: Behavioral data. Behavioural Brain Research. 1988; 31(1):47–59. DOI: 10.1016/0166-4328(88)90157-X [PubMed: 3228475]

Findeis MA. The role of amyloid β peptide 42 in Alzheimer's disease. Pharmacology & Therapeutics. 2007; 116(2):266–286. [PubMed: 17716740]

Foster DJ, Wilson MA. Hippocampal theta sequences. Hippocampus. 2007; 17(11):1093–1099. DOI: 10.1002/hipo.20345 [PubMed: 17663452]

Gallagher M, Koh MT. Episodic memory on the path to Alzheimer's disease. Current Opinion in Neurobiology. 2011; 21(6):929–934. DOI: 10.1016/j.conb.2011.10.021 [PubMed: 22079495]

Galloway CR, Lebois EP, Hernandez NH, Shagarabi SL, Manns JR. Effects of selective allosteric activation of M1 and M4 muscarinic receptors on object recognition memory performance in rats. Pharmacology. 2014; 93:57–64. DOI: 10.1159/000357682 [PubMed: 24480931]

Gómez-Isla T, Price JL, McKeel DW Jr, Morris JC, Growdon JH, Hyman BT. Profound loss of layer II entorhinal cortex neurons occurs in very mild Alzheimer's disease. Journal of Neuroscience. 1996; 16(14):4491–4500. [PubMed: 8699259]

Good MA, Hale G, Staal V. Impaired "episodic-like" object memory in adult APPswe transgenic mice. Behavioral Neuroscience. 2007; 121(2):443–448. DOI: 10.i1037/0735-7044.121.2.443 [PubMed: 17469935]

Griffin AL, Hallock HL. Hippocampal signatures of episodic memory: Evidence from single-unit recording studies. Frontiers in Behavioral Neuroscience. 2013; 7(54):1–8. DOI: 10.3389/fnbeh.2013.00054 [PubMed: 23423702]

Hall AM, Roberson ED. Mouse models of Alzheimer's disease. Brain Research Bulletin. 2012; 88(1):3–12. [PubMed: 22142973]

Hampstead BM, Stringer AY, Stilla RF, Amaraneni A, Sathian K. Where did I put that? Patients with amnestic mild cognitive impairment demonstrate widespread reductions in activity during the encoding of ecologically relevant object-location associations. Neuropsychologia. 2011; 49(9):2349–2361. DOI: 10.1016/j.neuropsychologia.2011.04.008 [PubMed: 21530556]

Hanaki R, Abe N, Fujii T, Ueno A, Nishio Y, Hiraoka K, … Mori E. The effects of aging and Alzheimer's disease on associative recognition memory. Neurological Sciences. 2011; 32(6): 1115–1122. DOI: 10.1007/s10072-011-0748-4 [PubMed: 21904867]

Hanes J, Zilka N, Bartkova M, Caletkova M, Dobrota D, Novak M. Rat tau proteome consists of six tau isoforms: implication for animal models of human tauopathies. Journal of Neurochemistry. 2009; 108(5):1167–1176. DOI: 10.1111/j.1471-4159.2009.05869.x [PubMed: 19141083]

Huxter J, Burgess N, O'Keefe J. Independent rate and temporal coding in hippocampal pyramidal cells. Nature. 2003; 425(6960):828–832. DOI: 10.1038/nature02058 [PubMed: 14574410]

Jeffery KJ. Integration of the sensory inputs to place cells: What, where, why, and how? Hippocampus. 2007; 17(9):775–785. DOI: 10.1002/hipo.20322 [PubMed: 17615579]

Kessels RP, Rijken S, Banningh LWJW, Van Schuylenborgh-VAN Es N, Rikkert MGO. Categorical spatial memory in patients with mild cognitive impairment and Alzheimer dementia: Positional versus object-location recall. Journal of the International Neuropsychological Society. 2010; 16(1): 200–204. DOI: 10.1017/S1355617709990944 [PubMed: 19883520]

Knierim JJ, Lee I, Hargreaves EL. Hippocampal place cells: Parallel input streams, subregional processing, and implications for episodic memory. Hippocampus. 2006; 16(9):755–764. [PubMed: 16883558]

Kukull WA, Higdon R, Bowen JD, McCormick WC, Teri L, Schellenberg GD, … Larson EB. Dementia and Alzheimer disease incidence: A prospective cohort study. Archives of Neurology. 2002; 59(11):1737–1746. DOI: 10.1001/archneur.59.11.1737 [PubMed: 12433261]

Lasztóczi B, Klausberger T. Hippocampal place cells couple to three different gamma oscillations during place field traversal. Neuron. 2016; 91:34–40. DOI: 10.1016/j.neuron.2016.05.036 [PubMed: 27387648]

Lavenex P, Amaral DG. Hippocampal-neocortical interaction: A hierarchy of associativity. Hippocampus. 2000; 10(4):420–430. [PubMed: 10985281]

Lebois EP, Bridges TM, Lewis LM, Dawson ES, Kane AS, Xiang Z, … Niswender CM. Discovery and characterization of novel subtype-selective allosteric agonists for the investigation of M1 receptor function in the central nervous system. ACS Chemical Neuroscience. 2009; 1:104–121.

Lebois EP, Digby GJ, Sheffler DJ, Melancon BJ, Tarr JC, Cho HP, Lindsley CW. Development of a highly selective, orally bioavailable and CNS penetrant M1 agonist derived from the MLPCN probe ML071. Bioorganic & Medicinal Chemistry Letters. 2011; 21(21):6451–6455. DOI: 10.1016/j.bmcl.2011.08.084 [PubMed: 21930376]

Lebois EP, Schroeder JP, Esparza TJ, Bridges TM, Lindsley CW, Conn PJ, … Levey AI. Disease-modifying effects of M1 muscarinic acetylcholine receptor activation in an Alzheimer's disease mouse model. ACS Chemical Neuroscience. 2017; 8(6):1177–1187. DOI: 10.1021/acschemneuro.6b00278 [PubMed: 28230352]

Lebois EP, Trimper JB, Hu C, Levey AI, Manns JR. Effects of selective M1 muscarinic receptor activation on hippocampal spatial representations and neuronal oscillations. ACS Chemical Neuroscience. 2016; 7(10):1393–1405. DOI: 10.1021/acschemneuro.6b00160 [PubMed: 27479319]

Leutgeb S, Leutgeb JK. Pattern separation, pattern completion, and new neuronal codes within a continuous CA3 map. Learning & Memory. 2007; 14(11):745–757. DOI: 10.1101/lm.703907 [PubMed: 18007018]

Levey AI, Kitt CA, Simonds WF, Price DL, Brann MR. Identification and localization of muscarinic acetylcholine receptor proteins in brain with subtype-specific antibodies. The Journal of Neuroscience. 1991; 11(10):3218–3226. [PubMed: 1941081]

Llorens-Martín M, Blazquez-Llorca L, Benavides-Piccione R, Rabano A, Hernandez F, Avila J, DeFelipe J. Selective alterations of neurons and circuits related to early memory loss in Alzheimer's disease. Frontiers in Neuroanatomy. 2014; 8(38):1–12. DOI: 10.3389/fnana.2014.00038 [PubMed: 24523676]

Mably AJ, Gereke BJ, Jones DT, Colgin LL. Impairments in spatial representations and rhythmic coordination of place cells in the 3xTg mouse model of Alzheimer's disease. Hippocampus. 2017; 27(4):378–392. [PubMed: 28032686]

Manns JR, Eichenbaum H. A cognitive map for object memory in the hippocampus. Learning & Memory. 2009; 16(10):616–624. DOI: 10.1101/lm.1484509 [PubMed: 19794187]

Manns JR, Howard MW, Eichenbaum H. Gradual changes in hippocampal activity support remembering the order of events. Neuron. 2007; 56(3):530–540. DOI: 10.1016/j.neuron.2007.08.017 [PubMed: 17988635]

McMillan P, Korvatska E, Poorkaj P, Evstafjeva Z, Robinson L, Greenup L, Leverenz J, Schellenberg GD, D'souza I. Tau isoform regulation is region-and cell-specific in mouse brain. Journal of Comparative Neurology. 2008; 511(6):788–803. DOI: 10.1002/cne.21867 [PubMed: 18925637]

Mitra PP, Pesaran B. Analysis of dynamic brain imaging data. Biophysical Journal. 1999; 76(2):691–708. DOI: 10.1016/S0006-3495(99)77236-X [PubMed: 9929474]

Mizuseki K, Royer S, Diba K, Buzsáki G. Activity dynamics and behavioral correlates of CA3 and CA1 hippocampal pyramidal neurons. Hippocampus. 2012; 22(8):1659–1680. DOI: 10.1002/hipo.22002 [PubMed: 22367959]

Morrissette DA, Parachikova A, Green KN, LaFerla FM. Relevance of transgenic mouse models to human Alzheimer disease. Journal of Biological Chemistry. 2009; 284(10):6033–6037. DOI: 10.1074/jbc.R80003020 [PubMed: 18948253]

Moser EI, Kropff E, Moser MB. Place cells, grid cells, and the brain's spatial representation system. Annual Review of Neuroscience. 2008; 31(1):69–89. DOI: 10.1146/annurev.neuro.31.061307.090723

Noebels J. A perfect storm: Converging paths of epilepsy and Alzheimer's dementia intersect in the hippocampal formation. Epilepsia. 2011; 52(s1):39–46. DOI: 10.1111/j.1528-1167.2010.02909.x

Oakley H, Cole SL, Logan S, Maus E, Shao P, Craft J, … Berry R. Intraneuronal β-amyloid aggregates, neurodegeneration, and neuron loss in transgenic mice with five familial Alzheimer's disease mutations: Potential factors in amyloid plaque formation. Journal of Neuroscience. 2006; 26(40):10129–10140. [PubMed: 17021169]

O'Keefe J, Dostrovsky J. The hippocampus as a spatial map. Preliminary evidence from unit activity in the freely-moving rat. Brain Research. 1971; 34(1):171–175. DOI: 10.1016/0006-8993(71)90358-1 [PubMed: 5124915]

O'Keefe J, Nadel L. The hippocampus as a cognitive map. Oxford: Oxord UP; 1978.

O'Keefe J, Recce ML. Phase relationship between hippocampal place units and the EEG theta rhythm. Hippocampus. 1993; 3(3):317–330. [PubMed: 8353611]

Oliva A, Fernández-Ruiz A, Buzsáki G, Berényi A. Spatial coding and physiological properties of hippocampal neurons in the Cornu Ammonis subregions. Hippocampus. 2016; 26(12):1593–1607. DOI: 10.1002/hipo.22659 [PubMed: 27650887]

Palop JJ, Chin J, Roberson ED, Wang J, Thwin MT, Bien-Ly N, … Finkbeiner S. Aberrant excitatory neuronal activity and compensatory remodeling of inhibitory hippocampal circuits in mouse models of Alzheimer's disease. Neuron. 2007; 55(5):697–711. DOI: 10.1016/j.neuron.2007.07.025 [PubMed: 17785178]

Querfurth HW, LaFerla FM. Mechanisms of disease: Alzheimer's disease. New England Journal of Medicine. 2010; 362(4):329–344. DOI: 10.1056/NEJMra0909142 [PubMed: 20107219]

Rubio SE, Vega-Flores G, Martínez A, Bosch C, Pérez-Mediavilla A, del Río J, … Pascual M. Accelerated aging of the GABAergic septohippocampal pathway and decreased hippocampal rhythms in a mouse model of Alzheimer's disease. The FASEB Journal. 2012; 26(11):4458–4467. [PubMed: 22835830]

Save E, Poucet B, Foreman N, Buhot MC. Object exploration and reactions to spatial and nonspatial changes in hooded rats following damage to parietal cortex or hippocampal formation. Behavioral Neuroscience. 1992; 106(3):447. [PubMed: 1616611]

Schomburg EW, Fernández-Ruiz A, Mizuseki K, Berényi A, Anastassiou CA, Koch C, Buzsáki G. Theta phase segregation of input-specific gamma patterns in entorhinal-hippocampal networks. Neuron. 2014; 84:470–485. DOI: 10.1016/j.neuron.2014.08.051 [PubMed: 25263753]

Skaggs WE, McNaughton BL, Wilson MA, Barnes CA. Theta phase precession in hippocampal neuronal populations and the compression of temporal sequences. Hippocampus. 1996; 6(2):149–172. DOI: 10.1002/(SICI)1098-1063(1996)6:2<149::AID-HIPO6>3.0.CO;2-K [PubMed: 8797016]

Steward O, Scoville SA. Cells of origin of entorhinal cortical afferents to the hippocampus and fascia dentata of the rat. Journal of Comparative Neurology. 1976; 169(3):347–370. [PubMed: 972204]

Terry RD, Masliah E, Salmon DP, Butters N, DeTeresa R, Hill R, … Katzman R. Physical basis of cognitive alterations in Alzheimer's disease: Synapse loss is the major correlate of cognitive impairment. Annals of Neurology. 1991; 30(4):572–580. DOI: 10.1002/ana.410300410 [PubMed: 1789684]

Thomé A, Gray DT, Erickson CA, Lipa P, Barnes CA. Memory impairment in aged primates is associated with region-specific network dysfunction. Molecular psychiatry. 2015; 21(9):1257–1262. DOI: 10.1038/mp.2015.160 [PubMed: 26503764]

Trimper JB, Galloway CR, Jones AC, Mandi K, Manns JR. Gamma oscillations in rat hippocampal subregions dentate gyrus, CA3, CA1, and subiculum underlie associative memory encoding. Cell Reports. 2017; 21:2419–2432. DOI: 10.1016/j.celrep.2017.10.123 [PubMed: 29186681]

Trimper JB, Stefanescu RA, Manns JR. Recognition memory and theta–gamma interactions in the hippocampus. Hippocampus. 2014; 24(3):341–353. DOI: 10.1002/hipo.22228 [PubMed: 24227610]

Vemuri P, Jack CR. Role of structural MRI in Alzheimer's disease. Alzheimer's Research & Therapy. 2010; 2(4):23.doi: 10.1186/alzrt47

Wilson IA, Ikonen S, Gallagher M, Eichenbaum H, Tanila H. Age-associated alterations of hippocampal place cells are subregion specific. The Journal of Neuroscience. 2005; 25(29):6877–6886. DOI: 10.1523/JNEUROSCI.1744-05.2005op [PubMed: 16033897]

Witter MP, Wouterlood FG, Naber PA, Van Haeften T. Anatomical organization of the parahippocampal-hippocampal network. Annals of the New York Academy of Sciences. 2000; 911(1):1–24. DOI: 10.1111/j.1749-6632.2000.tb06716.x [PubMed: 10911864]

Yassa MA. Ground zero in Alzheimer's disease. Nature Neuroscience. 2014; 17(2):146–147. DOI: 10.1038/nn.3631 [PubMed: 24473258]

Zhao R, Fowler SW, Chiang AC, Ji D, Jankowsky JL. Impairments in experience-dependent scaling and stability of hippocampal place fields limit spatial learning in a mouse model of Alzheimer's disease. Hippocampus. 2014; 24(8):963–978. DOI: 10.1002/hipo.22283 [PubMed: 24752989]

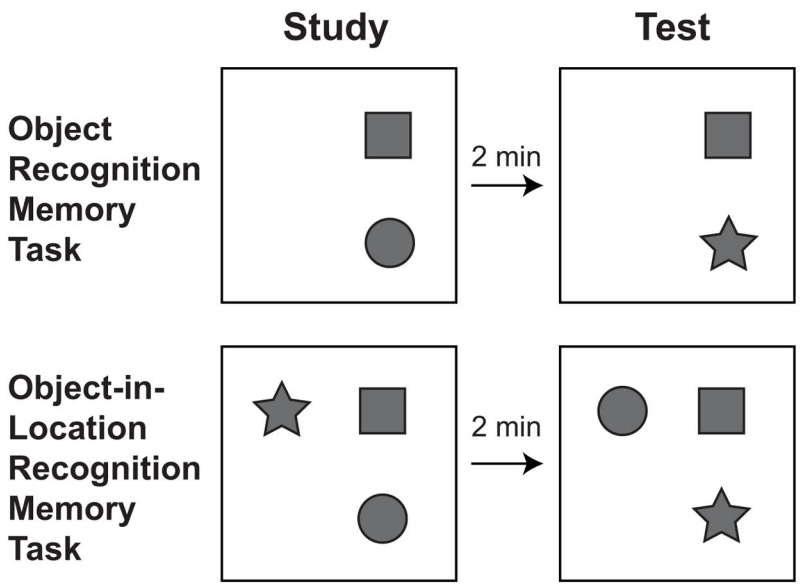

Figure 1.

Schematic of procedures for the object and object-in-location recognition memory tasks. Each trial of both tasks included a study phase and a test phase. For the object recognition memory task, rats encountered two novel objects during the study phase, then a duplicate of one of the study objects and a different novel object during the test phase. For the object-in-location memory task, rats encountered three novel objects during the study phase and three duplicates of the study phase objects during the test phase. One duplicate was placed in the same location as it appeared during the study phase, and two duplicates swapped locations. Rats completed two trials of each task each month from 5 to 12 months of age. Unique novel objects were used for each trial, and locations were counterbalanced across trials (see Materials and Methods for details).

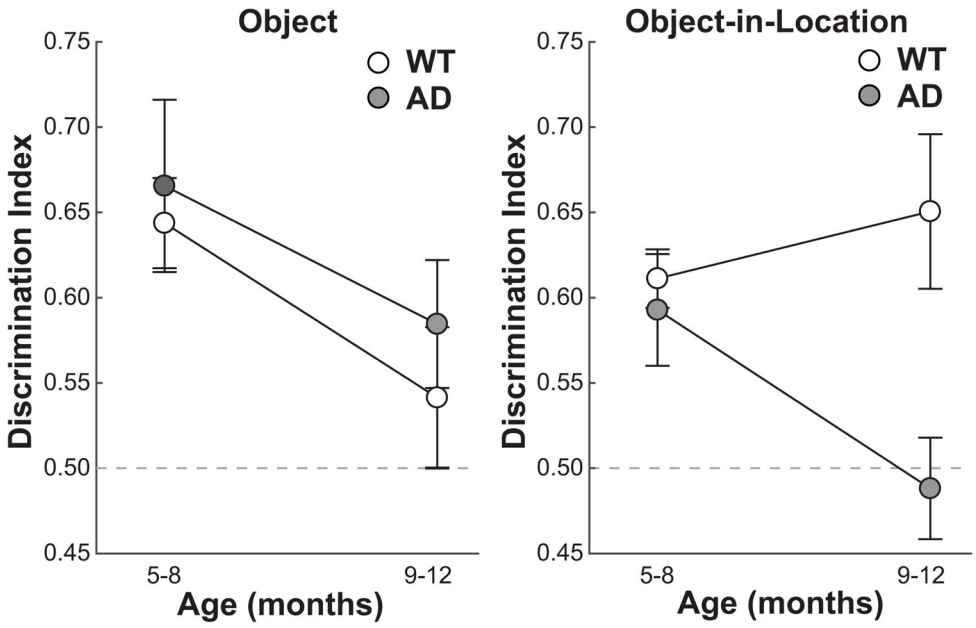

Figure 2.

Recognition memory performance on an object recognition memory task (left panel) and an object-in-location recognition memory task (right panel) at different age ranges. The results are shown as mean Discrimination Index (DI) across WT (n = 8) and AD (n = 8) rats. Error bars show ± *SEM*. The dashed line indicates chance performance. AD rats showed impaired object-in-location memory performance relative to WT rats by 9–12 months of age.

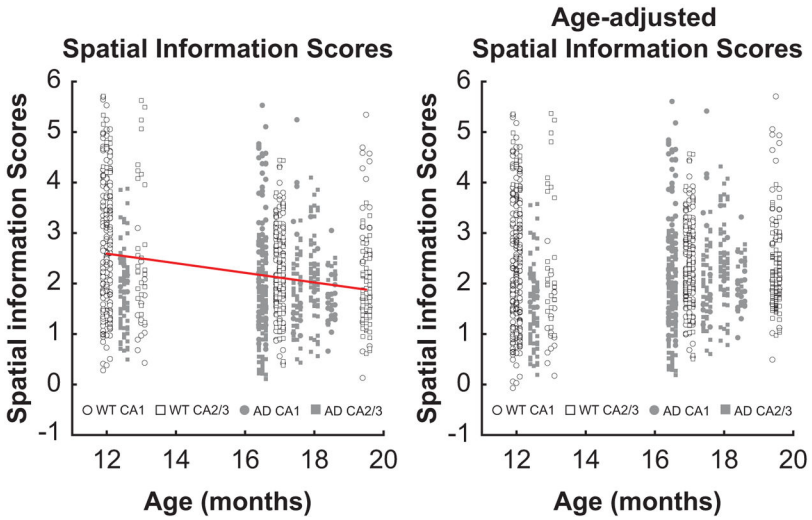

Figure 3.

Spatial information scores of CA1 and CA2/3 hippocampus place cells in WT and AD rats plotted by age. Spatial information scores correlated with age (left-panel), and adjusting spatial information scores for age caused spatial information scores of units recorded from older rats to be higher.

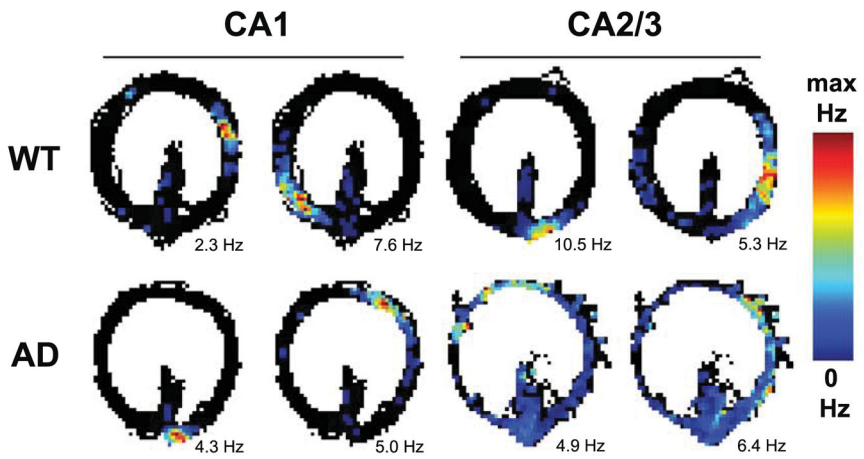

Figure 4.

Example place cells recorded from WT and AD rats in hippocampal regions CA1 or CA2/3. The examples were taken from the control (no drug) condition. The color bar indicates the colors used to plot firing rates across locations of the circle track. Maximum firing rates are noted below each example. The examples depict that CA2/3 place cells (but not CA1 place cells) in AD rats showed less spatial specificity as compared to place cells in WT rats.

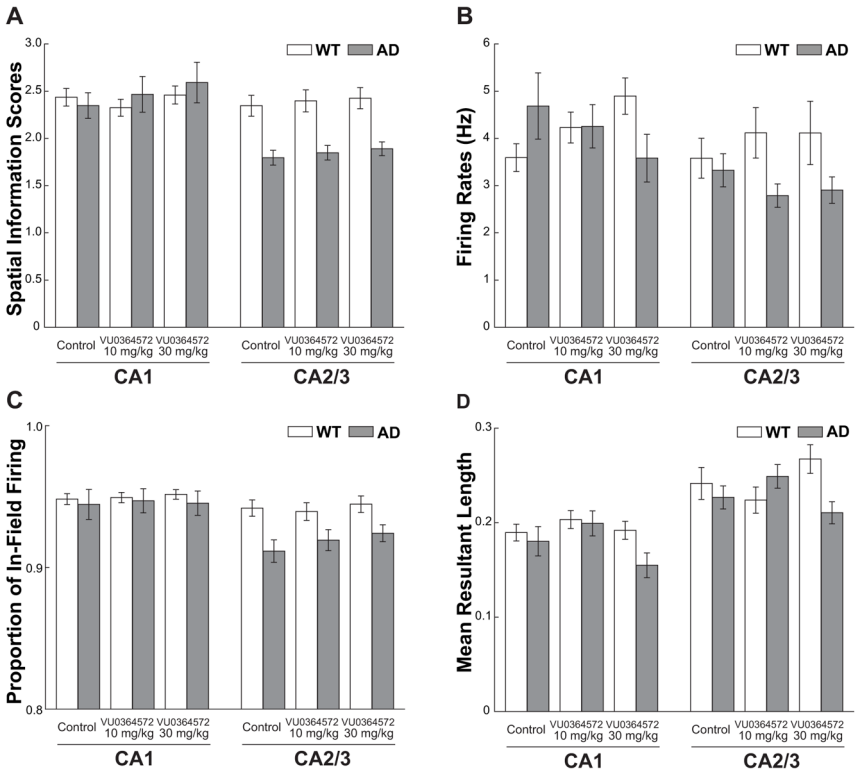

Figure 5.

Spatial information scores, in-field firing rates, proportion of in-field firing, and mean resultant length of CA1 and CA2/3 hippocampal place cells in WT and AD rats. Results are shown as age-adjusted mean scores across neurons in the control (vehicle only), 10 mg/kg, and 30 mg/kg M_1 mAChR agonist VU0364572 conditions. **A.** Spatial information scores. Place cells of AD rats showed reduced spatial information scores relative to those of WT rats, particularly in the CA2/3 region across all drug conditions (region by genotype interaction, $p < 0.001$; see Results). **B.** In-field firing rates. Relative to the control condition, oral administration of VU0364572 decreased in-field firing rates of AD hippocampal place cells yet increased in-field firing rates of WT hippocampal place cells (drug condition by genotype interaction, $p < 0.05$; see Results). **C.** Proportion of in-field firing. Place cells of AD rats showed lower proportions of in-field firing relative to those of WT rats, particularly in the CA2/3 region across all drug conditions (region by genotype interaction, $p < 0.001$; see Results). **D.** Mean resultant length of spikes relative to phase of theta oscillations. Administration of VU0364572 influenced the magnitude of theta phase modulation of spiking differently for AD and WT rats (drug condition by genotype interaction, $p<0.05$; see Results). In each panel, error bars show ± *SEM.* As an additional way of viewing the results, Supplementary Figure 1 replots the data from AD rats in panels A–D as a normalized (Z scored) difference from WT data within each drug condition.

Table 1

Numbers of hippocampal pyramidal cells recorded and labeled as place cells

		CA1			CA2/3		
		control	VU0364572 10 mg/kg	VU0364572 30 mg/kg	control	VU0364572 10 mg/kg	VU0364572 30 mg/kg
Pyramidal cells	**WT**	172	174	174	100	101	83
	AD	51	45	45	146	127	161
Place cells	**WT**	143	145	142	75	80	69
	AD	43	41	39	117	103	115

Table 2

Characteristics of hippocampal place cells

		CA1			CA2/3		
		control	**VU0364572 10 mg/kg**	**VU0364572 30 mg/kg**	**control**	**VU0364572 10 mg/kg**	**VU0364572 30 mg/kg**
Place Field Area (cm.^{2})	**WT**	**683.25** (±30.35)	**678.55** (±28.01)	**670.93**(±28.63)	**537.83**(±36.49)	**650.22** (±44.26)	**602.08**(±36.80)
	AD	**736.07** (±61.30)	**779.42** (±59.38)	**701.14**(±53.69)	**754.28** (±79.83)	**688.76** (±39.70)	**688.80**(±39.06)
Number of Place Fields per Cell	**WT**	**1.15**(±0.03)	**1.17**(±0.03)	**1.24** (±0.04)	**1.21** (±0.05)	**1.11**(±0.03)	**1.14**(±0.05)
	AD	**1.13**(±0.05)	**1.32** (±0.09)	**1.13** (±0.06)	**1.22** (±0.05)	**1.31** (±0.06)	**1.18** (±0.04)

Table 3

EEG power (mean dB ± SEM) recorded from pyramidal layers of CA1 and CA3

	CA1			CA3		
	control	VU0364572 10 mg/kg	VU0364572 0 mg/kg	control	VU0364572 0 mg/kg	VU0364572 30 mg/kg
WT theta	**28.82**(±0.91)	**28.96**(±0.911)	**29.31**(±0.99)	**28.74**(±1.03)	**28.61**(±0.85)	**29.07**(±0.95)
AD theta	**28.63**(±1.32)	**28.88**(±1.66)	**28.49**(±1.56)	**29.01**(±0.79)	**29.37**(±0.71)	**28.87**(±1.06)
WT slow gamma	**12.04**(±0.66)	**12.00**(±0.54)	**12.18**(±0.49)	**16.72**(±1.19)	**16.65**(±1.10)	**16.79**(±1.16)
AD slow gamma	**10.72**(±0.70)	**10.75**(±0.76)	**11.04**(±0.65)	**15.89**(±0.93)	**15.94**(±0.89)	**16.00**(±0.82)
WT fast gamma	**6.86**(±0.79)	**6.92**(±0.69)	**7.01**(±0.71)	**10.79**(±1.06)	**10.79**(±1.00)	**11.04**(±1.09)
AD fast gamma	**4.64**(±1.07)	**4.83**(±1.04)	**5.69**(±0.85)	**9.92**(±0.56)	**9.88**(±0.47)	**9.94**(±0.45)